Physics of resonant tunneling. The one-dimensional double-barrier case

B. Ricco* and M. Ya. Azbel†
IBM Thomas J. Watson Research Center, Yorktown Heights, New York 10598
(Received 21 September 1983)

In this work we discuss how the occurrence of resonant tunneling through a one-dimensional (1D) double barrier involves some interesting phenomena which have so far been overlooked. The effect of an externally applied electric field is considered, and it is shown that with fully symmetrical barriers it leads to weaker resonances than otherwise possible. Furthermore, the time required for resonance to be fully established is discussed, and it is shown that, depending on the barrier transmission coefficients and experimental conditions, it can be exceedingly long, thus contributing to a reduction of resonance effects on the usual experimental time scale. We also show that resonant tunneling under the usual experimental conditions implies carrier trapping, hence a buildup of space charge available for modifying the potential-energy barrier. Different current behaviors then result from the inherent feedback mechanism. The effects of temperature on the measured current are finally discussed.

I. INTRODUCTION

In this paper, we discuss in some detail the problem of resonant tunneling through a one-dimensional (1D) double (potential energy) barrier. Pioneering work on this subject is primarily due to Esaki, Chang and Tsu[1] who used GaAs-$Ga_{1-x}Al_xAs$ heterostructures, and to Hirose *et al.*[2] who, instead, worked on the Si-SiO_2 system. From a theoretical point of view significant contributions came from J. C. Penley[3] and Sandomirskii in the 60's while recently new experiments were performed by Sollner *et al.*[4] and by Ricco *et al.* on double barrier grown by means of molecular-beam epitaxy.

The purpose is primarily that of showing how, although the occurrence of resonances is a simple and well-known result of the usual treatment of tunneling, it involves some complicated physical effects which have so far been almost completely overlooked. The failure to fully understand the importance of such effects and the consequent lack of attention to their regard might, in our opinion, explain the only partial success of the pioneering experimental work[1,2] aimed at showing resonant tunneling. Although truly remarkable these works share the rather unpleasant characteristic of finding effects much weaker and less pronounced than expected from the theory. This implicitly suggested the idea that resonant tunneling is too critically dependent on experimental parameters to be really controllable and (re)producible, let alone exploited, in real life where samples' or devices conditions' (defect concentration, surface cleanliness, actual dimensions, etc.) are of course different from the clear-cut exact pictures of theoretical models.

Although differences between theory and experiments are certainly to be expected, we feel that the criticality of resonant tunneling has been, and still is, overestimated and that the somewhat disappointing experimental results might well be due to nonoptimal samples and measurement conditions.

Recently,[4] new experiments carried out on GaAs-$Ga_{1-x}Al_xAs$ double barriers similar to those of Ref. 1 have produced *I-V* characteristics with well pronounced peaks. The key factor for the improvement seems here to be the better material quality available today. From a quantitative point of view, the improvement over previous experiments is relevant (a 6:1 ratio between peaks and valleys is observed) but a large discrepancy still exists with theoretical predictions. As will be shown in this paper this cannot, at least in part, be considered surprising since in almost all respects, these experiments are similar to those of Ref. 1.

Two points, in particular, are important and will be dealt with in this paper. First, while the measurements have been carried out with a nonnegligible electric field applied across the double barrier, the assumed underlying theory did not include it.[2,5] The most important remark with respect to this is that the electric field destroyed the symmetry of the two realized barriers and, consequently, contributed significantly to reduce the effects of resonances. As will be shown later, better structures than those used so far can be designed to maximize resonance peaks but it is essential to take into account the effects of the field. This involves some nontrivial engineering. Futhermore, because the field cancels the intrinsic simple symmetry, the optimization can only be performed for one of the possible several peaks.

A second important point to grasp about the experiment is that because of the way they were realized the occurrence of substantial effects is not an immediate phenomenon. Resonant tunneling is time dependent and, to be fully established, requires a non-negligible time (exponentially long as will be explained later). Therefore, if the experiments feature ramping voltages and no care is taken to allow for enough time at the peaks, resonance effects might well be almost completely lost.

A further remark concerns the space-change buildup necessarily taking place because of the accumulation of

tunneling carriers within the resonant well which, to all practical purposes, behaves as a dynamic trap (in the sense that particles continuously get in and out of it). Since the accumulating charge modifies the potential-energy barriers a feedback mechanism becomes operational and complicates the resonance time evolution as well as the engineering for optimized experiments. In particular it will be shown that, if the amount of charge that can be trapped into the well is substantial, oscillating currents as well as self-accelerating approaches to "stationary states" are possible.

In this paper we will also briefly consider the effects of temperature which, when increasing, can lead to decreasing as well as increasing currents depending on the relative position of Fermi level and resonance states.

Before tackling these points, in Sec. III, the method based on the transfer-matrix technique will be presented which allows an explict, easy treatment of the 1D double barrier case with no restriction on the shape of the potential-energy diagram. Futhermore, in Sec. II a brief account is given in the known simplest case of square barriers, usually treated in textbooks, which provides a good starting point for our subsequent generalizations.

II. CASE OF RECTANGULAR BARRIERS

The case of two rectangular potential-energy barriers (such as depicted in Fig. 1) is the most elementary example where resonant tunneling occurs. Futhermore, it presents the advantage of exact analytical solutions. For these reasons, it can be found in textbooks and will be only briefly reviewed here to be used as a guideline for the most direct understanding of the major features of resonant tunneling. As will be shown later, all the concepts encountered in doing so can be generalized to the most general case of double barriers of any shape.

For the potential-energy diagram of Fig. 1, the global transmission coefficient T_G of the whole barrier (i.e., from points H and A) can be exactly derived[6] and put in the following general form:

$$T_G=\frac{C_0}{C_1T_lT_r+C_2\frac{T_l}{T_r}+C_3\frac{T_r}{T_l}+C_4\frac{1}{T_lT_r}}\ , \tag{1}$$

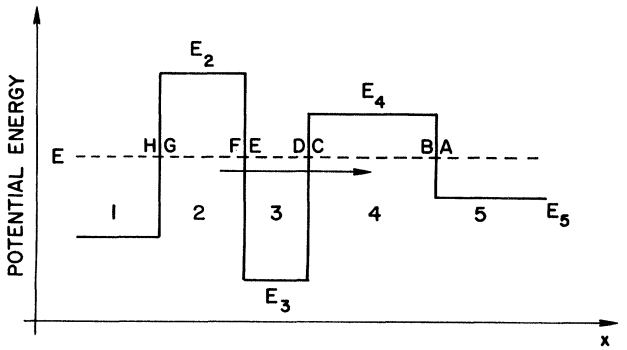

FIG. 1. Potential-energy diagram of the double rectangular barrier case.

where T_l and T_r represent the transmission coefficients of the left and right barrier, respectively (namely those between point G-F and C-B) which are exponentially dependent on energy. In Eq. (1) the C's are (phase) factors exhibiting a much weaker energy dependence and, at first order, can essentially be treated as constants (of the same order of magnitude). We will only consider here the case of "strong localization" (the meaning of this term will become clear later) which requires all T's to be small ($\ll 1$). Under this condition, the denominator of Eq. (1) is dominated by the last term and it is

$$T_G\approx\frac{C_0}{C_4}T_lT_r\approx T_lT_r\ . \tag{2}$$

In this case then, the presence of the potential-energy well between the two barriers has, in practice, little or no effect depending upon the way one looks at the global barrier. In particular, everything goes as points E and D in Fig. 1 were coincident and no well was present; or, alternatively, if seen without joining such points, the only effect produced by the well is a reduction of the (phase) area of the total barrier.

For some special energies, however, C_4 goes to zero; the leading term is, consequently, canceled out and a resonance occurs. In this case, as easily seen from Eq. (1), the global transmission coefficient $T_{G\,\mathrm{res}}$ becomes

$$T_{G\,\mathrm{res}}\approx C\frac{T_{\min}}{T_{\max}}\approx\frac{T_{\min}}{T_{\max}}\ , \tag{3}$$

where $T_{\min}$ and $T_{\max}$ represent the smaller and larger among T_l and T_r, respectively, while C is either C_0/C_2 or C_0/C_3 depending on whether or not $T_{\max}=T_l$.

By directly comparing Eqs. (2) and (3) it is obvious that a resonance always implies an increasd transmission coefficient since it is

$$T_{G\,\mathrm{res}}/T_{GN}=1/T_{\max}^2 \tag{4}$$

where T_{GN} represents the "normal" value T_G would have without resonance, i.e., if no well was present between the two barriers of Fig. 1. Such as increase is, therefore, larger for smaller $T_{\max}$ and vanishes in the limiting case of $T_{\max}\to 1$ (which, on the other hand, is incompatible with the assumption of strong localization).

The result expressed in Eq. (3) [and, consequently, in Eq. (4)] holds even when the internal energy well is very narrow (provided certain conditions to be specified below are met). This offers the best opportunity to illustrate a first important, general concept, namely that, while the presence of the well has scarcely any effect off resonance, it can dramatically alter the tunneling probability throughout the global barrier at special energies. In particular, Eq. (3) shows that regardless of how small T_l and T_r are, $T_{G\,\mathrm{res}}$ can be of order of unity under the only condition $T_l=T_r$ while Eq. (4) clearly indicates that the transmission coefficient can easily increase at several orders of magnitude for arbitrarily small changes in energy producing resonance.

For C_4 to vanish, hence resonance to take place, the only condition to be satisfied from a physical point of view is that the energy (E) of the tunneling carrier(s)

matches that (E_s) of the well (quasi) eigenstates. In mathematical terms, this can be expressed as[7]

$$k_3 d_3 = \tan^{-1}\frac{\alpha_2}{k_3} + \tan^{-1}\frac{\alpha_4}{k_3} + (n-1)\pi \ . \tag{5}$$

In Eq. (5) $k_i = \hbar^{-1}[2m(E-E_p)]^{1/2}$ and $\alpha_i = \hbar^{-1}[2m(E_p - E)]^{1/2}$ (here E_p denotes the potential energy) are used to indicate the action absolute value in classically allowed and forbidden regions, respectively (this notation will be maintained throughout the present work).

Another important aspect of resonance concerns the wave function as schematically represented in Fig. 2. In essence, without resonance the wave function $\phi(x)$ monotonically and exponentially decreases within the classically forbidden regions thus reflecting the multiplication of the single-barrier transmission coefficients of Eq. (2).

At resonance, instead, the tunneling particle finds "its" (eigen)state in the well where, consequently, the wave function has to be peaked with an exponential decrease on both sides (see Fig. 2). Since we assumed both T_l and $T_r \ll 1$, this implies that the state is strongly localized (hence the name of the assumption made earlier). Because T_l and T_r are not zero, the localized states are, strictly speaking, quasi eigenstates with a finite lifetime and energy width as described later. The assumption of strong localization, however, implies they can be considered as "real" eigenstates to all practical purposes. In the case of $T_l < T_r$ considered in Fig. 2, it is immediately evident that the total transmission coefficient is given by the ratio of those of the single barriers (T_l/T_r) as expressed by Eq. (3).[8]

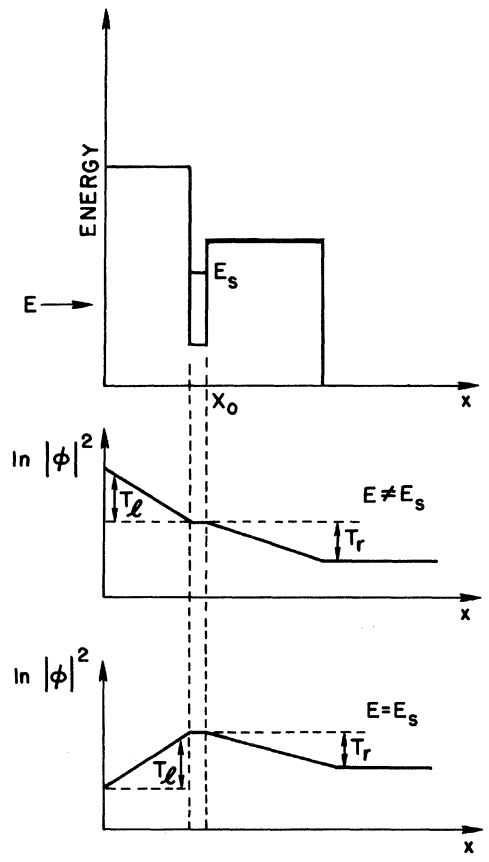

FIG. 2. Schematic representation of the wave function "at" and "off" resonance.

A point is immediately suggested in Fig. 2 and is worth mentioning in anticipation of later discussions. The increase in transmission coefficient at resonance is a consequence of the wave function being peaked within the well. Furthermore, Fig. 2 describes a stationary situation since it is based on the results of the time-independent Schrödinger equation. Hence, when starting with electrons only present to the left of the global barrier (i.e., of point H in Fig. 1) a transient is in order before any resonance can be fully established. In this process, probability density has to accumulate within the well which, therefore, behaves as a trap for the incoming (tunneling) particle(s). In the final, resonant state, the well is then responsible for both carrier trapping and high current (throughout the whole system) and the two effects, far from contrasting with each other as it might seem at first, are in fact complementary. The key factor for this is, of course, that carrier retention (trapping) within the well is a dynamic process where particles get in and out of the well at any time. In the steady state, in particular, the incoming and outgoing fluxes must be the same.

When dealing with charged carriers (only electrons will be considered hereafter), the trapping process mentioned above implies a charge buildup which, in turn, modifies the problem potential energy. The amount of charge (or particle) that the well can accommodate depends on the wave-function localization, hence on the single-barrier transmission coefficient and, more specifically, on $T_{\max}$. When such an amount is substantial, carrier trapping has at least two important consequences.

First, the potential energy to enter the Schrödinger equation must be calculated self-consistently, i.e., accounting for the contribution due to electron trapping. This complicates the calculations and has bearings on the conditions for resonances: In particular, for instance, even barriers intended to be rectangular are not really so and, consequently, an approach suitable for a more general potential is required. Second, during the transients leading to the final situation, a feedback mechanism becomes operative, since the barriers change as particles accumulate into the well. This modifies the resonance time evolution. As will be discussed later, either self-accelerating approaches to a stationary state, or unstable, oscillating currents are possible depending on the carrier energy at the cathode.

III. THE CASE OF A GENERAL POTENTIAL THE TRANSFER-MATRIX TECHNIQUE

The best way to obtain the results of the preceding section in a form which can be easily generalized to any potential-energy diagram is to use the transfer-matrix technique.[9] With reference to Fig. 1 this requires the knowledge of four different types of matrices, namely, those respectively joining points: within classically allowed regions ($D \rightarrow E$), below a barrier ($B \rightarrow C$ and

$F \rightarrow G$), across a discontinuity from below to outside a barrier ($A \rightarrow B$, $E \rightarrow F$), and across a discontinuity in the opposite direction ($G \rightarrow H$, $C \rightarrow D$). These matrices will hereafter be denoted with $\underline{M}_A$, $\underline{M}_B$, $\underline{M}_{\text{out}}$, and $\underline{M}_{\text{in}}$, respectively. By including in the wave-function coefficient (at each point) a factor accounting for a shift of origin to that point and using for k and α the notation introduced just after Eq. (5), these matrices have the following expressions:

$$\underline{M}_A = \begin{bmatrix} e^{-ikw} & 0 \\ 0 & e^{ikw} \end{bmatrix}, \tag{6a}$$

$$\underline{M}_B = \begin{bmatrix} e^{-\alpha w} & 0 \\ 0 & e^{\alpha w} \end{bmatrix}, \tag{6b}$$

$$\underline{M}_{\text{out}} = \frac{1}{2} \begin{bmatrix} 1+i\frac{k}{\alpha} & 1-i\frac{k}{\alpha} \\ 1-i\frac{k}{\alpha} & 1+i\frac{k}{\alpha} \end{bmatrix}, \tag{6c}$$

$$\underline{M}_{\text{in}} = \frac{1}{2} \begin{bmatrix} 1-i\frac{\alpha}{k} & 1+i\frac{\alpha}{k} \\ 1+i\frac{\alpha}{k} & 1-i\frac{\alpha}{k} \end{bmatrix}. \tag{6d}$$

In Eqs. (6a) and (6b), w represents the distance between the points to be connected.

It is worth pointing out, before proceeding, that the above matrices are particular cases of more general forms which can be derived by exploiting the wave-function properties with respect to conjugation and conservation of probability current.[9] Considering these properties, the matrix $\underline{M}_A$ connecting points ($T \rightarrow V$) within classically allowed regions can be set in the form

$$\underline{M}_A = \left[\frac{k_v}{k_t}\right]^{1/2} \begin{bmatrix} \cosh S\, e^{-i\delta} & \sinh S\, e^{i\beta} \\ \sinh S\, e^{-i\beta} & \cosh S\, e^{i\delta} \end{bmatrix}, \tag{7a}$$

where S, δ, and β are three real parameters characterizing the region between the connected points. In particular if this includes a barrier, S represents its phase area while δ and β are phase factors depending on the choice of coordinate reference.[10]

Much in the same way, it can be shown that when the points to be connected belong to classically forbidden regions $\underline{M}_B$ can be put in the form

$$\underline{M}_B = \left[\frac{\alpha_t}{\alpha_v}\right]^{1/2} \begin{bmatrix} \cosh S\, e^{\delta} & \sinh S\, e^{\beta} \\ \sinh S\, e^{-\beta} & \cosh S\, e^{-\delta} \end{bmatrix}, \tag{7b}$$

where again S, δ, and β are three real parameters.

The case of matrices, such as $\underline{M}_{\text{in}}$ and $\underline{M}_{\text{out}}$, connecting points in qualitatively different regions, is slightly more complicated. In both cases, taking the conjugate wave functions, it can be shown that the matrices have the general form

$$\underline{M}_{\text{in,out}} = \begin{bmatrix} M_{11} & M_{11}^* \\ M_{22}^* & M_{22} \end{bmatrix}. \tag{7c}$$

(Here the asterisk indicates the complex conjugate.) Furthermore, conservation of the probability current gives

$$M_{11}M_{22} - M_{11}^* M_{22}^* = \begin{cases} i\frac{k}{\alpha} \\ \frac{\alpha}{ik} \end{cases}, \tag{7d}$$

where the upper and lower right-hand results apply when going from a classically allowed to a forbidden region and in the opposite direction, respectively.

Once the matrices given in Eqs. (6) are known, the $\underline{M}_{\text{tot}}$ for the total barrier (i.e., connecting point A to H of Fig. 1) is easily worked out since

$$\underline{M}_{\text{tot}} = \underline{M}_{GH}\underline{M}_{FG}\underline{M}_{EF}\underline{M}_{DE}\underline{M}_{CD}\underline{M}_{BC}\underline{M}_{AB} . \tag{8}$$

The global transmission coefficient T_G is then simply given by

$$T_G = 1/|(\underline{M}_G)_{11}|^2 . \tag{9}$$

By using the technique briefly described above, the case of a general potential-energy function $E_p(x)$ can now easily be tackled under the conditions for the quasiclassical approximation to be applicable (see, for instance, Ref. 11, page 164). In particular if, as a first step, we maintain the discontinuities of Fig. 1 but let $E_p(x)$ be general in the intervals G-F, E-D, and C-B, the treatment outlined so far still holds provided the elements of $\underline{M}_A$ and $\underline{M}_B$ are replaced by the quasiclassical expressions, namely

$$\left.\begin{matrix} (\underline{M}_A)_{11} \\ (\underline{M}_A)_{22} \end{matrix}\right\} = \exp \mp i \int k(x)dx , \tag{10}$$

where $k(x) = \hbar^{-1}\{2m[E - E_p(x)]\}^{1/2}$ and the integral is calculated between the points to be connected (i.e., the classical turning points at the well edges). Similarly,

$$\left.\begin{matrix} (\underline{M}_B)_{11} \\ (\underline{M}_B)_{22} \end{matrix}\right\} = \exp\left[\mp \int \alpha(x)dx\right],$$

where

$$\alpha(x) = \hbar^{-1}\{2m[E_p(x) - E]\}^{1/2} . \tag{11}$$

As a result, the condition for resonance (implicitly determining the resonant energy) expressed by Eq. (5) simply becomes

$$\int k(x)dx = \tan^{-1}\frac{\alpha_l}{k_l} + \tan^{-1}\frac{\alpha_r}{k_r} + (n-1)\pi , \tag{12}$$

where the integral is calculated between the well classical turning points at which the parameters appearing on the right-hand side are also taken (here l and r indicate the left- and right-well edge, respectively).

A conceptually more complicated problem arises when at least one of the discontinuities is removed since at turning points such as those represented by Fig. 3 the (continuous) potential energy equals that of the tunneling particle [i.e., $E_p(x) = E$] and the quasiclassical approximation cannot be used as such. These points require special care as discussed in Ref. 11 (p. 169) where connecting formulas consistent with the quasiclassical approximation and suitable for this case are derived. Such an approach, however, needs a slight improvement to be used in conjunction with the transfer-matrix technique since it seems insufficiently

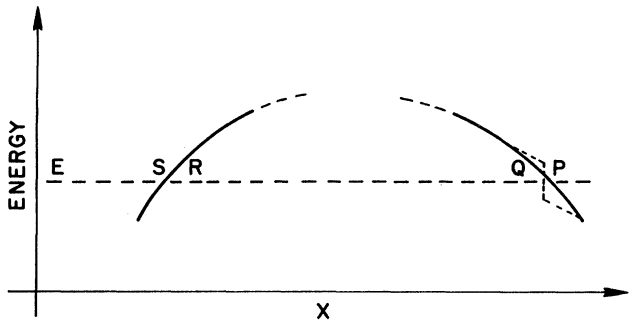

FIG. 3. Continuous turning points.

accurate to deal with both independent solutions of Schrödinger equation on both sides of the considered point. In particular the derived connecting formulas only provide the (1,2)th and (2,2)th elements of the $\underline{M}_{\text{in}}$ (or $\underline{M}_{\text{out}}$) matrix. We can, however, exploit the general property expressed by Eq. (7c) to easily construct the whole matrix with no loss of accuracy.

When crossing takes place without discontinuities, we then obtain[12]

$$\underline{M}_{\text{out}}=\frac{1}{\sqrt{2}}\begin{bmatrix}1+i & 1-i\\ 1-i & 1+i\end{bmatrix}, \tag{13a}$$

$$\underline{M}_{\text{in}}=\frac{1}{\sqrt{2}}\begin{bmatrix}1-i & 1+i\\ 1+i & 1-i\end{bmatrix}. \tag{13b}$$

As for the conditions providing resonance energies, Eq. (12) still holds with $\alpha_i/k_i=1$; hence $\tan^{-1}(\alpha_i/k_i)=\pi/4$ for the turning point(s) where $E=E_p(x)$.

The equation can, in fact, be put in a very compact form covering the cases where the turning point(s) are either "continuous" or feature a discontinuity with $E_p(x)\to\infty$ (infinite wall with $\alpha\to\infty$). From Eq. (12) we have

$$\int\{2m[E-E_p(x)]\}^{1/2}dx=\tfrac{1}{2}(n-\gamma)h\ , \tag{14}$$

where the integral is calculated throughout the well, n is an integer and

$$\gamma=\begin{cases}0 \text{ for (infinite) walls on both well edges,}\\ \frac{1}{4} \text{ for one wall and one continuous edge,}\\ \frac{1}{2} \text{ for two continuous edges.}\end{cases}$$

Equations (12) and (14) implicitly provide an estimate of the resonance energies with the accuracy of the semiclassical approximation which, therefore, increases with n (namely when the resulting energy increases with respect to h).

Another important feature of resonances is that the peaks they produce in the transmission coefficient (hence in measured currents) have a finite energy width ΔE which is physically due to the nonzero probability to tunnel out of the well. As known, such a width is related to the (resonant) state lifetime. For the reason given above ΔE increases with the electron escape probability, thus essentially with $T_{\max}$, namely,

$$\Delta E\propto T_{\max}\ . \tag{15}$$

From a mathematical point of view, Eq. (15) can be derived by looking at Eq. (1) and finding the energy at which the two leading terms in the denominator have comparable (actually equal) absolute value. From Eq. (54) of Ref. 6, this gives

$$\left[\frac{1}{T_{\min}T_{\max}}\sin w_1\right]^2=\left[\frac{T_{\max}}{T_{\min}}\sin w_2\right]^2 \tag{16}$$

with $w_2\neq w_1$ and $\sin w_1=0$ at resonant energy E_0. Rearranging Eq. (16), expanding up to first order in energy about E_0, i.e., making $E=E_0+\Delta E$,

$$\left[\frac{\sin w_1}{\sin w_2}\right]^2=T_{\max}^4\ ,$$
$$(T_{\max}^4)_{E=E_0}+4(T_{\max}^3)_{E=E_0}\Delta E=0 \tag{17}$$

and the linear relationship of Eq. (15) immediately follows.

The finite width of the resonance peaks plays a relevant role in experiments. First of all it makes less critical the energy matching condition required to produce a resonance (although, of course, the effects decrease away from the peak centers). Furthermore, in the case where the tunneling electrons are nonmonochromatic, i.e., they are spread over a whole energy range within the cathode, the larger a peak width, the larger is the fraction of particles taking part in resonant tunneling. Under this condition, assuming that the electron distribution can be considered constant over the whole ΔE, the current contribution due to a resonant peak is essentially given by

$$J_{\text{res}}\propto T_{\max}\frac{T_{\min}}{T_{\max}}\ , \tag{18}$$

where the first term accounts for the fraction of electrons involved and the second represents the global transmission coefficient at resonances. Without resonance the same amount of carriers would produce a current J_{off} given by

$$J_{\text{off}}\propto T_{\max}^2T_{\min}\ . \tag{19}$$

It is then immediately obvious that resonance can give rise to an extremely large current increase. In particular, with the notation used above, it is

$$\frac{J_{\text{res}}}{J_{\text{off}}}=\frac{1}{T_{\max}^2}\ . \tag{20}$$

IV. CASE OF DOUBLE BARRIER WITH AN APPLIED FIELD

A case of special interest from the point of view of experiments is that of a double barrier subject to an externally applied electric field. The structures which have been used so far[1,2,4] feature barriers with the same technological parameters (height and width) as shown in Fig. 4(a).

In the case of no field ($F=0$) using the notation of Fig. 4(a), resonances would occur at energies satisfying Eq. (12) which becomes

$$\frac{1}{\hbar}\sqrt{2m}Ew=2\tan^{-1}\frac{(\Phi_0-E)^{1/2}}{E^{1/2}}+(n-1)\pi\ . \tag{21}$$

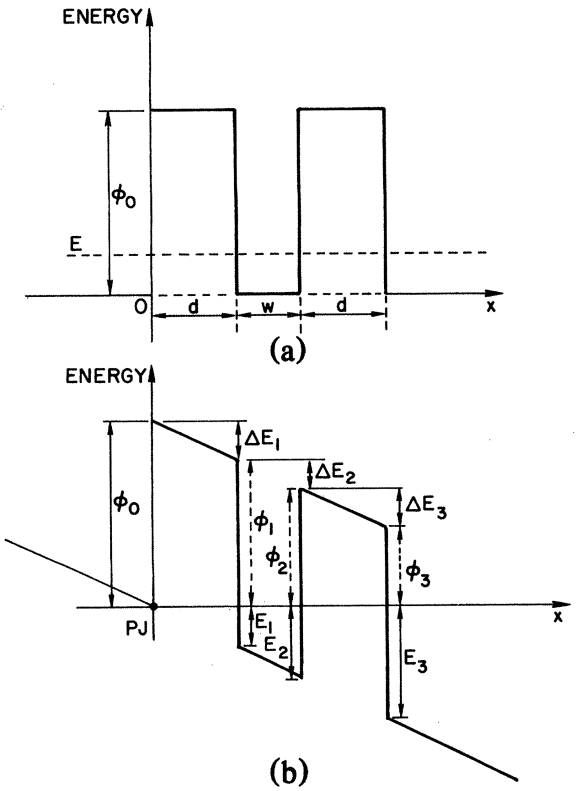

FIG. 4. (a) Symmetrical double barrier (no field applied). (b) Double barrier with applied field (no longer symmetrical).

The special characteristics of this case is that, because of the symmetry embedded in the structure, at any of such energies the global transmission coefficient T_G would be of the order of 1 regardless of the values chosen for the barrier and well parameters. This makes the engineering of the sample to be used particularly simple although it must be realized that some important experimental features do depend on such parameters. This is, for instance the case for the increase in transmission coefficient which becomes larger if the single barriers are made less transparent [Eq. (4)]. Furthermore, carrier trapping (and the consequent feedback mechanism already mentioned) as well as the time constants required to fully establish a resonance are also affected. These considerations suggest the need for thoughtful choice of structure parameters, but do not alter the conclusion that structural symmetry is "the" condition to realize when looking for resonant tunneling in the case of no, or rather negligible, fields.

The kind of experiments outlined above, however, requires the possibility to change the energy of the tunneling carriers so that the current ($\propto T_G$) versus energy curves showing resonance peaks can be worked out.

In practice, the simplest and most commonly used experimental setup is one where the tunneling carriers come from a semiconductor (or metal) cathode. Although their energy can be increased (for instance by using temperature or light), it is more convenient to act on the well eigenstates bringing them down to the same level of the carriers by applying a voltage V_a across the structure. Under this condition, tunneling essentially occurs at the (fixed) energy of the cathode conduction-band bottom (or Fermi level with metals) and J vs V_a (rather then J vs E) is measured. Overall the energy diagram pertinent to such a problem is schematically represented in Fig. 4(b) where PJ indicates the point at which tunneling essentially takes place. (In this we neglect, for simplicity, the contribution coming from carriers at a slightly higher energy in the cathode which can, at first order, be accounted for by adjusting the barrier height Φ_0).

Such a technique, however, implies the use of relevant fields and these drastically change the experimental conditions. A first, important effect which is immediately apparent in Fig. 4(b) is that the applied voltage destroys the symmetry of the barriers whose transmission coefficients are no longer equal. In particular it is

$$T_l=\exp\left[-\frac{4}{3}\frac{1}{\hbar}\sqrt{2m}\,\frac{\Phi_0^{3/2}-\Phi_1^{3/2}}{qF_b}\right] \tag{22a}$$

and

$$T_r=\exp\left[-\frac{4}{3}\frac{1}{\hbar}\sqrt{2m}\,\frac{\Phi_2^{3/2}-\Phi_3^{3/2}}{qF_b}\right]. \tag{22b}$$

Here the subtracting term in the exponent becomes zero for triangular (rather than trapezoidal) barriers. In our case, of course, only the barrier on the right can be triangular. In Eq. (22)

$$\begin{aligned}\Phi_1&=\Phi_0-\Delta E_1=\Phi_0-qF_bd\ ,\\ \Phi_2&=\Phi_0-\Delta E_1-\Delta E_2=\Phi_0-q(F_bd+F_ww)\ ,\\ \Phi_3&=\Phi_0-\Delta E_1-\Delta E_2-\Delta E_3=\Phi_0-q(2F_bd+F_ww)\ ,\end{aligned} \tag{23}$$

where F_b and F_w represent the electric field in the barrier and well regions, respectively, and it is

$$F_b=V_a/(2d+w\epsilon_b/\epsilon_w),\quad F_w=\epsilon_bF_b/\epsilon_w\ . \tag{24}$$

Here ϵ_b and ϵ_w denote the dielectric constants of the barrier and well material while d and w denote the barrier and well width, respectively.

Since it is $T_l<T_r$, we have

$$\frac{T_{\min}}{T_{\max}}=\exp\left[-\frac{4}{3}\frac{d}{\hbar}\sqrt{2m}\times\frac{1}{qF_b}(\Phi_0^{3/2}-\Phi_1^{3/2}-\Phi_2^{3/2}+\Phi_3^{3/2})\right]. \tag{25}$$

This equation, which holds for any value of V_a, indicates that the transmission coefficient T_G obtainable at resonance cannot be too close to unity. In particular, for instance, for the case considered in Fig. 2 of Ref. 1 with $V_a=0.35$ V it is $T_{\min}/T_{\max}\approx10^{-4}$ and this implies a 4 order-of-magnitude reduction in the effects at resonance with respect to the optimal possible condition. (The case

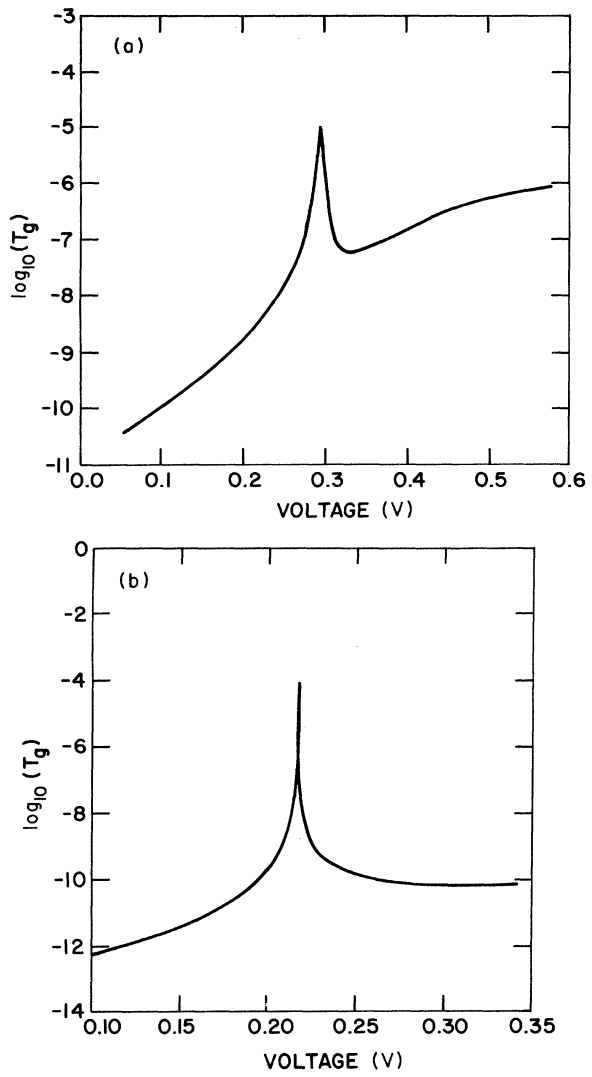

FIG. 5. Calculated transmission coefficient for the cases of Refs. 1(a) and 3(b).

of Ref. 2 is even worse in this respect.)

Figure 5(a) shows the transmission coefficient T_G for such a case calculated by means of the transfer-matrix technique outlined previously and good agreement is found both with the T_G value at the peak (not fully resolved in the figure because of the voltage scale) calculated analytically from Eq. (25) and with the experimental resonance voltage. Figure 5(b) shows, instead, the calculation for the case of Ref. 4 and the agreement with experiments is excellent as far as the voltage at which resonance occurs is concerned.

An important point to be made with regard to the above discussion is that by using a nonsymmetrical structure with the left barrier thinner than the right one, the condition for $T_l = T_r$ might be recreated thus enhancing the effects looked for in experiments. There are, however, two qualitative differences with the symmetrical, zero-field case already discussed: The possibility to realize the optimized condition (i.e., $T_G \approx 1$) is not guaranteed and, even if this can be achieved, it would be true only for a particular resonance peak (hence voltage).

To see this point in some more detail let us consider Eq. (25). For a given set (P) of technological parameters (Φ_0, d_l, w, and d_r where d_l and d_r indicate the thickness of the left and right barrier, respectively, and w the well width) we can try to solve (25) for the voltage V_a (entering the equation through F_b), giving $T_{\min} = T_{\max}$. Depending on the chosen set of parameters, this problem may or may not have a solution and overall it defines a function $V_a'(P)$ and a domain where such a function exists.

Although the obtained voltages are those at which the two barriers (defined by the parameters P) are functionally equal (i.e., $T_l = T_r$) they may not necessarily give rise to a resonance peak. In the way to be discussed just below, another function $V_a''(P)$ can be defined for the voltages at which resonances occur. The optimized experimental conditions can then be realized if the two functions V_a' and V_a'' intersect and the intersections define the structure to be used.

As already anticipated, such optimized conditions do not always exist, their search involves some not-straightforward engineering and, in any case, they are specific of a given resonance peak. In this sense the situation is just opposite to that of the zero-field case.

As for the voltages at which resonance occurs, the function $V_a''(P)$ defined above can be obtained by solving Eq. (12) which, in the case under consideration, becomes

$$\frac{1}{\hbar}\sqrt{2m}\,\frac{2}{3}\,\frac{E_2^{3/2}-E_1^{3/2}}{qF_w} = \tan^{-1}\frac{\Phi_1}{E_1}+\tan^{-1}\frac{\Phi_2}{E_2}+(n-1)\pi\,, \tag{26}$$

where the notation is that of Fig. 4(b) and

$$E_1 = \Delta E_1 = qF_b d_1\,, \qquad E_2 = E_1 + \Delta E_2 = q(F_b d_l + F_w w)\,. \tag{27}$$

As already mentioned the agreement with the experiments of Ref. 4 is excellent since we get $V_a = 0.21$ V. For the cases of Figs. 1 and 2 of Ref. 1, Eq. (26) gives $V_a = 0.22$ and 0.3 V, respectively, as positions of the lowest resonance peak. No higher peak, however, can be found since when $V_a \gtrsim 0.6$ the second barrier disappears (i.e., $\Phi_2 < 0$). Those shown in the mentioned reference can only be justified by assuming a large voltage drop due to series resistance (so that the actual voltage applied across the double barrier is actually lower) or invoking other phenomena. Among these, resonant tunneling via defect-related states of the type suggested and discussed in Ref. 13 might provide a reasonable explanation.

V. TIME DEVELOPMENT OF RESONANT TUNNELING

As already anticipated, a crucial aspect usually overlooked in experiments is that, depending on the initial conditions, a non-negligible time might be required before a high-conductivity resonant state is fully established.

In this respect, it is, perhaps, worth stressing again that

the analysis of Sec. II is based on the solutions of the time-independent Schrödinger equation hence describes a stationary situation. This, in turn, requires the carrier wave function at resonance to be (strongly) localized within the well (to a degree which decreases with increasing $T_{\max}$). The mentioned condition on the wave function is, in other words, necessary and sufficient for $T_{G\,\mathrm{res}}$ to be $\approx T_{\min}/T_{\max}$.

From a physical point of view such a requirement means that the carrier(s) must be predominantly localized (trapped) within the well or, equivalently, that this must be "filled up" with them (up to the level described by the stationary wave function) before resonant tunneling is fully established. In many experiments, however, this might well not correspond to actual initial conditions as is, in particular, the case of Refs. 1, 2, and 4 where the well eigenstates are initially above the energy level of the available carriers, hence completely empty. Under this condition, a transient with time constant τ_0 is required for the system to approach its final configuration. During such a transient, the incoming (tunneling) particles get essentially trapped within the well where probability density accumulates thus also making the global transmission coefficient to gradually increase.

The time constant τ_0 must, in general, be expected to depend on the initial condition (which might feature a steady flux or a single carrier with well-defined or spread-out energy). It can, in principle, be calculated by expanding the initial wave function in terms of the eigenfunctions of the double barrier Hamiltonian (and subsequently, using the superposition of time-dependent states) but a detailed calculation of this kind is here deferred to future work.

On physical grounds, however, we believe τ_0 to be of the order of the resonant state lifetime, hence to exponentially increase with the barrier phase area. In particular, we expect

$$\tau_0 \approx \frac{\hbar}{\Delta E} \propto \frac{1}{T_{\max}} . \tag{28}$$

Depending on the value of $T_{\max}$, τ_0 can assume non-negligible and even very large (exponentially large) values. This, in turn, would have killing effects on experiments where the resonant state is initially empty and is not given enough time to capture the due amount of carriers. As far as, in particular, the experiments of Refs. 1, 4, and 2 are concerned, this is not the case for Refs. 1 and 4 where the peak width is of the order of 10^{-4} eV and consequently $\tau_0 \approx 10^{-11}$ sec. In the case of Ref. 2, however, because of the much higher barrier height, $T_{\max}$ is several orders of magnitude lower and a rough estimate gives at low voltages $\tau_0 \approx 10^{6}$ sec.

Still with regard to the times involved in resonant tunneling it is also worth mentioning that if (or once) the eigenstate has all the carriers it can accomodate, a much shorter time τ_t becomes important, namely that required to cross the double barrier. As far as this is concerned, we expect τ_t to be essentially the time required to cross a single barrier according to the physical picture of carriers entering the filled state hence "pushing" others out on the other side of the double barrier. With barrier heights of order of few eV (or substantial fraction of eV) and width of tens of Å, τ_t is of the order of 10^{-13}–10^{-15} sec and therefore almost completely negligible.

For a more formal derivation of the previous time estimates, we can use the results of Refs. 14 and 15 where expressions for the traversal and dwell times through little transparent barriers are presented.

The dwell time represents the average time spent by an electron in a considered region and can, therefore, provide a good measure of our τ_0 when applied to the whole double barrier (assumed to extend from point G to A in Fig. 1). It is then

$$\tau_0 \approx J^{-1} \int_G^A |\Psi|^2 dx , \tag{29}$$

where J denotes the probability current through the double barrier.

As for the transit time τ_t, it is obviously coincident, for all practical purposes, with the tranversal time of Ref. 14 which turns out to be longer for more transparent barriers. In our case, once the steady state is reached, the time limiting factor for the current comes from crossing the more transparent barrier (here assumed to be the right one which extends from C to A) and it is then

$$\tau_t = \int_C^A \frac{m}{\hbar} \frac{dx}{\alpha_r(x)} \tag{30}$$

where as usual $\alpha_r = \hbar^{-1}\sqrt{2m}\,[E_r(x)-E]^{1/2}$.

Since we are interested here only in first-order estimates, let us consider for simplicity the square barrier case of Fig. 1. From the results summarized in Fig. 2 it is then

$$|\Psi|^2 = \begin{cases} C^2, & x > A \\ C^2 e^{-2\alpha_r(x-A)}, & C < x < B \\ \dfrac{1}{T_{\max}} C^2, & E < x < D \\ \dfrac{1}{T_{\max}} C^2 e \alpha_l^{(x-F)}, & G < x < F \end{cases} \tag{31}$$

where C is an arbitrary normalization factor and $T_{\max} = T_r = e^{-2\alpha_r d_r}$ with d_r denoting the thickness of the right barrier. We can now easily calculate the numerator of Eq. (29) by dividing the interval in the two barriers and the well as follows:

$$\begin{aligned} \int_G^A |\Psi|^2 dx &= \int_G^F |\Psi|^2 dx + \int_F^D |\Psi|^2 dx + \int_D^A |\Psi|^2 dx \\ &= C^2 \left[\frac{1}{2\alpha_l T_{\max}} (1 - e^{-2\alpha_l d_l}) + \frac{w}{T_{\max}} + \frac{1}{2\alpha_r} (e^{-2\alpha_r d_r} - 1) \right] \approx \frac{C^2}{T_{\max}} \left[\frac{1}{2\alpha_l} + \frac{1}{2\alpha_r} + w \right] , \end{aligned} \tag{32}$$

where w represents the width of the central well. Since the transmitted current is given by

$$J=C^2\frac{\hbar}{m}k_A \ , \tag{33}$$

it is

$$\tau_0=\frac{1}{T_{\max}}\frac{m}{\hbar}\frac{1}{k_A}\left[\frac{1}{2\alpha_l}+\frac{1}{2\alpha_r}+w\right] . \tag{34}$$

From Eq. (30), instead, we have

$$\tau_t=\frac{m}{\hbar}\frac{1}{\alpha_r}d_r \ . \tag{35}$$

From this, it can be seen that for comparable values of α's, k's, and geometrical factors τ_0 and τ_t essentially differ for the factor $1/T_{\max}$ in agreement with what was discussed previously in this section.

Another interesting phenomenon concerning the resonance time dependence involves the effect of temperature. The key point is that the thermal motion of the atoms in any sample contributes in making the potential energy time dependent. As far as this effect is concerned, from a qualitative point of view different cases can be distinguished. If the variations of potential energy E_p are very small or/and very slow (compared to τ_0), then E_p can be considered not to depend on time to all practical purposes. Under this circumstances the considerations developed in this paper fully apply.

If, instead, E_p significantly varies in values on a time scale comparable or smaller than τ_0, then a more complicated analysis is required. Work aimed at exploring this aspect of resonant tunneling is now in progress.[16]

Overall we expect the temperature to give rise to a broadening of the resonance peaks and to a decrease in their effects on the current measured in experiments.

As a final comment to this section, it is perhaps worth anticipating that the described evolution of empty states toward their final condition may be substantially affected by the space-charge buildup inherent to the carrier accumulation taking place within the well. This can modify the potential-energy barrier with a feedback mechanism whose major resulting effects are described in the next section.

VI. THE EFFECTS OF SPACE-CHARGE BUILDUP DUE TO CARRIER TRAPPING

As already discussed, resonance implies the presence inside the well of a certain amount of carriers which, at least in the most common experimental situtations, are not there at the beginning. When dealing with electrons, this means that a space charge builds up. If the resonant eigenstate can accommodate enough charge this affects the potential energy making it time dependent and giving rise to a feedback mechanism linking the changes in potential energy with carrier trapping.

The amount of charge that a resonant state can contain depends, in general, on its degree of localization. This, in turn, essentially decreases with increasing $T_{\max}$ since, if we denote with $\Phi_{\min}$ and $\Phi_{\max}$ the wave function outside the double barrier (reaching the barrier of transmission coefficient $T_{\min}$ and $T_{\max}$, respectively), it is

$$\frac{|\Phi_{\min}|^2}{|\Phi_{\max}|^2}=\frac{T_{\min}}{T_{\max}} \ , \tag{36}$$

and, when $T_{\max}\gg T_{\min}$, $|\Phi_{\min}|$ becomes negligible. $T_{\max}$, then, controls the dominant part of Φ outside the barrier.

Let us denote with $L_{\max}$ and W the size of the region outside the double barrier (where Φ is not negligible) and the well width, respectively. If we deal with one particle, the fraction of captured carrier is essentially given by

$$f=\frac{W}{W+T_{\max}L_{\max}} \ . \tag{37}$$

If there are many particles incident on the barrier (say from the left) the question of exclusion arises, and it becomes important to evaluate the number N of system levels contained within the width ΔE_s of the resonant state. Denoting with ΔE_l the distance between the allowed level, it is

$$N=\frac{\Delta E_s}{\Delta E_l} \ . \tag{38}$$

The number $N_{\rm tr}$ of carriers trapped into the well is then essentially given by (here we assume all of the N level to be occupied)

$$N_{\rm tr}=Nf \ . \tag{39}$$

Indicating with L_T the total system dimensions (actually the region where Φ is not negligible), ΔE_l can be estimated as

$$\Delta E_l\approx h\frac{v_F}{L_T} \ , \tag{40}$$

where v_F is the electron Fermi velocity. From this, it is immediately obvious that for an unlimited system ($L_T\to\infty$ and the energy spectrum becomes a continuum) a resonant state with finite width can contain any number of particles. If L_T is finite, Eq. (38) has to be evaluated. For this we use the expression

$$\Delta E_s=T_{\max}h\nu \ , \tag{41}$$

where ν is the attempt-to-escape frequency relative to the central well. For a rough estimate we assume $\nu=v_F/w$. It is then

$$N=\frac{L_T}{w}T_{\max} \ . \tag{42}$$

A slightly different case, which is important because it occurs in the experiments mentioned in this paper, is that where the incoming particles comes from a cathode which essentially behaves as an infinite reservoir of carriers at different energies as schematically represented in Fig. 6. Here the appropriate boundary condition is that the density of carriers is kept fixed at the cathode. Two points are relevant. First only the electrons within the energy window of the eigenstate width play a role in trapping since the wave function of the others exponentially decreases

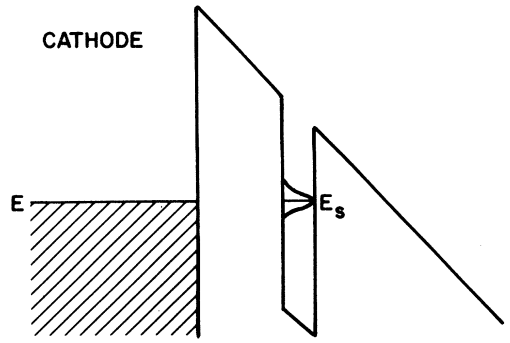

FIG. 6. Energy configuration under the usual experimental conditions.

below the first barrier and, consequently, their density in the well is negligible. Second, T_l (i.e., the transmission coefficient of the barrier facing the cathode) takes the place of T_{max} in the previous equations (regardless of whether or not $T_l = T_{max}$). States deep into the barrier, hence close to its boundary on the right of Fig. 6, produce slow (and little) trapping in spite of their T_{max} being high.

If the amount of charge contained in a well is not negligible at any given time the potential energy must be calculated in a self-consistent way, i.e., taking into account the contribution due to the trapped carriers.

There is, however, a point worth dealing with in some more details which concerns the way the system approaches the steady state (if this can ever be reached). From this point of view, we expect two different behaviors according to whether or not the incoming particles are monochromatic. In case they are, and their energy E is fixed, the (negative) space-charge buildup pushes the state energy E_s upward, thus breaking the energy matching condition for resonance. When this happens, the state starts losing its particle content (again with a transient on the time scale of its lifetime) thus being lowered in energy until $E = E_s$ again and resonance is restored. The net effect is, of course, that the system oscillates in time without ultimately reaching a stable steady state. The resulting oscillations (of frequency $\approx 1/\tau_0$ where τ_0 is the eigenstate lifetime) should be observable in the tunneling current in experiments where τ_0 is not negligibly small. These oscillations could also, perhaps, be exploited from a device point of view.

A completely different behavior must, instead, be expected in the case where the energy of the incoming particles covers the whole range swept by the rising E_s. (Naturally if this reaches and exceeds the upper limit of the tunneling carrier energy oscillations of the type described above are in order.) The dominant feature here is that resonance conditions are maintained as E_s moves and, consequently, the resonant state can keep increasing its charge content until it reaches a final steady configuration. As it does so, the charge buildup changes the potential-energy barriers on account of two different effects: It weakens and strengthens the field, respectively, on the left- and right-hand side of the well while, at the same time reducing the barrier heights (because E_s rises). In practice, the overall result is that both barriers become more transparent (i.e., T_l and T_r increase) as can, for instance, be schematically seen in Fig. 7. Here the well, and hence the trapped charge, has been replaced by a δ function while, for simplicty, the depth of the eigenstate has been kept fixed[17] (i.e., Φ_S is considered unchanged by the charge buildup) and it is evident that the barrier (phase) area can only decrease. This has two important consequences, namely, (i) the state degree of localization decreases (as T_{max} increases) thus decreasing the amount of charge the well can eventually accommodate, and (ii) for the same reason, the transient to reach the final stationary state becomes shorter [as indicated in Eq. (28)]. This latter effect is very important since it implies a self-accelerating (or positive feedback) mechanism in that as more charge is trapped into the well, trapping itself gets faster. If the final configuration is one of high conductivity the system will therefore, rapidly converge to it giving rise to abrupt, very large increase in tunneling current.

As described in Ref. 13, we believe this could be the way in which breakdown phenomena occurs in thin insulating films where only low voltages are required to reach the high fields causing the material failure.

VII. TEMPERATURE EFFECTS

In Sec. V we mentioned an interesting phenomenon relating the temperature (T) with resonance time evolution.

Here we consider instead the effect due to the electron thermal population and the important conclusion is reached that at resonance a variety of current-versus-T relationships can result depending on the relative position of the resonant state and the Fermi energy (E_F). In particular, currents increasing as well as decreasing with T and complicated nonmonotonic temperature behaviors are possible. Each state gives rise to its own (individual) J vs T dependence according to its energy position. In real samples where many such states are present, then a different (individual) current behavior is to be expected at each resonant peak. This is in agreement with experiments showing that the conductance at a peak is proportional to $\exp[(T_0/T)^{1/2}]$ where T_0 is individual for the considered

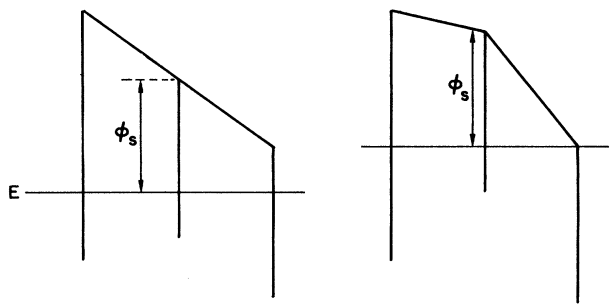

FIG. 7. Schematic representation of the charges on the potential energy induced by electron trapping.

peak.[18] The physical effects of concern of this section are essentially the following.

As the temperature varies the cathode carrier concentration at the resonant energy also varies and so does the current J measured in experiments. At the same time the carrier thermal velocity also increases with T and, with semiconductor or metal cathodes, this implies an increase in the electron flux hitting the barrier, hence J. This latter is, however, only a minor effect (because the thermal velocity depends on $\sqrt{T}$) with respect to that mentioned earlier whose temperature dependence comes from the exponential factor in the Fermi distribution function.

Because we essentially deal with the carrier concentration within a definite narrow energy window (the width of a resonant eigenstate centered on E_s) the effects to be expected depend on its position relative to E_s. If E_s and E_F are close (compared with kT) an increase of T spreading out the distribution function can only lead to a decrease of particle concentration at the resonance energy, hence to a decrease of tunneling current. In this case J exhibits a metallic type of behavior.

In any case, for large increase of temperature a subsequent increase in current may occur since, as the distribution function spreads out, the carrier concentration can become non-negligible at other, higher eigenstates whose contribution will rapidly become important. If, on the other hand, the distance between E_s and E_F is large, an increase in current is first expected to occur as a consequence of the increase in carrier concentration available for resonant tunneling. Here too, however, a subsequent metallic type of behavior can arise for the same reasons given above.

VIII. CONCLUSIONS

In this paper, we have presented an assessment of the basic physical phenomena involved in resonant tunneling through a one-dimensional double barrier structure. In particular we have shown that, although they are a straightfoward, well-known feature of the transmission coefficient versus energy (or field) characteristics, the occurrence of resonances involves interesting physical phenomena which complicate the search for experimental conditions able to emphasize their effects.

In this respect, we have shown that experiments performed on structures with semiconductor electrodes with varying applied voltages, can, at most, only be optimized for a particular resonance peak.

We have also pointed out that, under the most usual experimental conditions, a time-dependent process with non-negligible time constant is necessary to reach the steady state situation. At the beginning of the mentioned transient, the conductivity throughout the double barrier can be much lower than in the final state and this might explain some experimental results. Furthermore, we have discussed how at resonance carrier trapping (as well as high conductivity) occurs. This, in turn, brings about a space-charge effect making the potential-energy barrier time dependent. Because of this a feedback mechanism takes place and either a self-accelerating approach to an equilibrium state or a permanent oscillating current can result.

Finally the effect of temperature has been briefly treated and the conclusion is reached that metallic- as well as semiconductor-type behavior can be found.

---

*On leave from the University of Padua, 35100 Padua, Italy.
†On leave from the University of Tel Aviv, Tel Aviv 69978, Israel.

[1]L. L. Chang, L. Esaki, and R. Tsu, Appl. Phys. Lett. 24, 593 (1974).
[2]M. Hirose, M. Morita, and Y. Osaka, Jpn. J. Appl. Phys. 16, 561 (1977).
[3]J. C. Penley, Phys. Rev. 128, 596 (1962).
[4]T. C. L. G. Sollner, W. D. Goodhue, P. E. Tannenwald, C. D. Parker, and D. D. Peck, Appl. Phys. Lett. 43, 588 (1983).
[5]R. Tsu and L. Esaki, Appl. Phys. Lett. 22, 562 (1973).
[6]E. O. Kane, *Tunneling Phenomena in Solids,* edited by E. Burnstein and D. Lundquist (Plenum, New York, 1969).
[7]The last term in the equation differs by a factor of 2 from that of Ref. 6 [Eq. (61)] probably due to a misprint.
[8]It is perhaps worth mentioning that in the opposite case of $T_r < T_l$ the wave function of Fig. 2 does not represent an adequate description of the problem with electrons coming from the left (of point H in Fig. 1). This "boundary condition" can be dealt with by either of the following approaches. We can consider the dual case of particles coming from the right (of course completely symmetrical with respect to that of Fig. 2) and exploit the general property of transmission coefficients to be independent on the side the barriers are looked at. In such a way, the results follow immediately from that of Fig. 2. Alternatively, we can construct the wave function $\phi(x)$ appropriate to the case at hand by means of two independent solutions of Schrödinger equation. ϕ_1, represented in Fig. 2, can be used as one of them while the other, ϕ_2, can be worked out from it. In particular the most general wave function ϕ can be expressed in terms of ϕ_1 in the following way: $\phi = A\phi_1 + B\phi_1 \int 1/\phi_1^2 dx$, where A and B represent the coefficients of the linear combination ϕ must be constructed from.
[9]M. Ya. Azbel, Phys. Rev. B 28, 4106 (1983).
[10]The factor in front of the matrix is not present in Eqs. (7) because the carrier momentum does not change in a given region of Fig. 1. If, however, a global matrix for a barrier is constructed by taking $\underline{M}_{in}\underline{M}_{B}\underline{M}_{out}$ and the momentum on its sides is different, it can be easily seen that the resulting determinant is k_v/k_t. Consequently, the matrix can be put in the form given in Eq. (7a). The same applies in the case of Eq. 7(b).
[11]L. D. Landau and E. M. Liftshitz, *Quantum Mechanics,* 3rd ed. (Pergamon, Oxford, 1976).
[12]It is, perhaps, interesting to notice at this regard that the result coincides with that obtainable by arbitrarily introducing a discontinuity at the crossing point (symmetrical with respect to the energy of the tunneling particle to maintain $\alpha = k$ as in the real case—see dotted line in Fig. 3) and letting it go to zero. This procedure is, however, not completely rigorous.
[13]B. Ricco, M. Ya. Azbel, and M. H. Brodsky, Phys. Rev. Lett. 51, 1795 (1983).
[14]M. Büttiker and R. Landauer, Phys. Rev. Lett. 49, 1739 (1982).

[15]M. Büttiker, Phys. Rev. B 27, 6178 (1983).
[16]M. Ya. Azbel, P. A. Lee, and D. Stone (private communication).
[17]In reality, the position of the resonant level changes with field in the way implicitly described in Eq. (12). Here, however, a compensation occurs at first order between the weakening and strengthening field on the well sides.
[18]A. B. Fowler, A. Hartstein, and R. A. Webb, Phys. Rev. Lett. 48, 196, (1982); A. Hartstein, R. A. Webb, A. B. Fowler, and J. J. Wainer, in Proceedings of the Electronic Properties of Two-dimensional Systems, Oxford (U.K.), September, 1983 (unpublished).